

Helmut Eschrig

Leibniz-Institut für Festkörper- und Werkstofforschung Dresden

Leibniz-Institute for Solid State and Materials Research Dresden



High- T_c Superconductors: Electronic Structure

1. Introduction
2. The undoped cuprate
 - 2.1 CaCuO_2 as an $n = \infty$ model cuprate
 - 2.2 Angle resolved photoemission spectroscopy on $\text{Sr}_2\text{CuO}_2\text{Cl}_2$
3. Theoretical models
4. Doped cuprates
 - 4.1 Overdoped regions
 - 4.2 Bilayer splitting in $(\text{Bi,Pb})_2\text{Sr}_2\text{CaCu}_2\text{O}_{8+\delta}$
 - 4.3 Underdoped region
 - 4.4 Single-electron self-energy
5. Summary

This talk is based on a manuscript for an article in the

'Encyclopedia of Materials', edited by K.H.J. Buschow *et al.*, Elsevier, Oxford 2003.

Discussions with many colleagues have to be acknowledged, in particular

K. Koepernik
I. Chaplygin
H. Rosner
R. Hayn
S. Drechsler

L. Maksimov
A. Barabanov
N. Plakida
P. Fulde

J. Fink
M. Golden
S. Borisenko
G. Krabbes

W. Pickett
A. Shick
G. Sawatzky

P. Coleman
E. Müller-Hartmann
A. Aharony

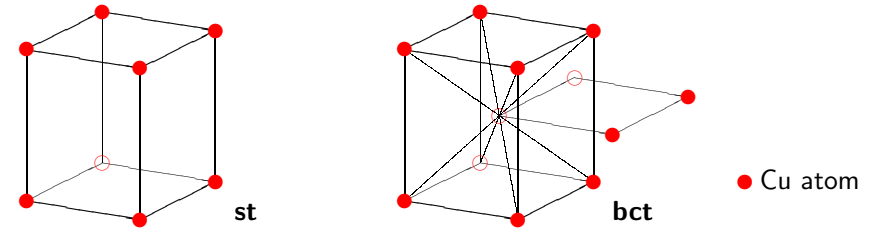
M. Eschrig

1. Introduction

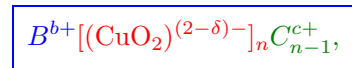
An understanding of the electronic structure of the High- T_c cuprate superconductors must start out from an analysis of their **chemical composition, valencies, structure and binding.**

All cuprate high- T_c superconductors are **stacks** of alternating **anionic CuO_2 layers** and **block layers** which are in gross cationic.

The stacking direction is commonly taken as the crystallographic c -direction and the crystal symmetry is generally derived from a **simple tetragonal (st)** or a **body-centered tetragonal (bct)** symmetry, although it is in fact often **orthorhombic** due to **distortions** or due to **vacancy ordering**.



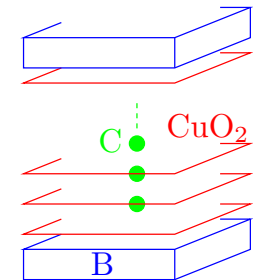
The general composition of the cuprate superconductors is



where

$n = 1, 2, 3 \dots$, $c = 2$ or 3 , $b = c + n(2 - \delta - c)$.

The block layer B is a cationic metal oxide layer.



It is followed by either a single $(\text{CuO}_2)^{(2-\delta)-}$ layer or a stack consisting of n such layers with cations C sandwiched in between.

So far, the cations C are Ca^{2+} , or RE^{3+} where $\text{RE} = \text{Y}$, La or any of the lanthanides.

The main families of cuprate superconductors:

(i) $\text{La}_{2-x}\text{Sr}_x\text{CuO}_{4-y}$

$(\text{La}_{2-x}\text{Sr}_x\text{O}_{2-y})^{(2-\delta)+}(\text{CuO}_2)^{(2-\delta)-}$ with $n = 1$ and $\delta \approx x$ for $y \approx 0$; related is $M_2\text{CuO}_2X_2$ or $(M_2X_2)^{(2-\delta)+}(\text{CuO}_2)^{(2-\delta)-}$ with $M = (\text{Ca}_{1-x}\text{Na}_x)$ or Sr and $X = \text{F, Cl or Br}$.

(ii) $\text{RE}_1\text{Ba}_2\text{Cu}_3\text{O}_{6+x}$

$(\text{Ba}_2^+(\text{CuO}_{2+x})^{(3+2\delta)-})[(\text{CuO}_2)^{(2-\delta)-}]_2\text{RE}^{3+}$ with $n = 2$ and $\delta = 0$ for $x < 0.3$ and then increasing to $\delta \approx 0.2$ for $x \approx 1$.

(iii) $B^{(2-n\delta)+}[(\text{CuO}_2)^{(2-\delta)-}]_n\text{Ca}_{n-1}^{2+}$, $n = 1, 2, 3, \dots$

$B = (\text{Bi,Pb})_2\text{Sr}_2\text{O}_{4+x}$ or $\text{TlBa}_2\text{O}_{2.5+x}$ or $\text{Tl}_2\text{Ba}_2\text{O}_{4+x}$ or $\text{HgBa}_2\text{O}_{2+x}$, and δ increases with increasing x ; Tl may be replaced by B and Hg by Cu or Au; Ca may be replaced by Y, Dy, Er.

The oxygen in the metal oxide block layers B is more or less volatile. Above, it is written in such a way that in all cases the doping level of the cuprate planes $\delta = 0$ for $x = 0$ or some value of x close to zero.

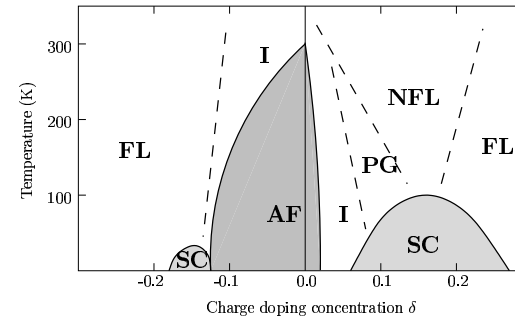
The metal oxide block layer B is, depending on composition and on x , either insulating or metallic.

The cation C is always fully ionized, its valence orbitals are unoccupied.

The essential conducting component which also carries superconductivity is the $(\text{CuO}_2)^{(2-\delta)-}$ layer which is doped by charge transfer to the block layer.

The doping level δ may be positive (hole doping) or negative (electron doping). Electron doping is less frequent and is found in particular in the family (i) with $B = (\text{Nd}_{2-x}\text{Ce}_x\text{O}_{2-y})$ or $B = (\text{Pr}_{2-x}\text{Ce}_x\text{O}_{2-y})$ instead of $(\text{La}_{2-x}\text{Sr}_x\text{O}_{2-y})$. The tetravalent Ce donates one electron.

Generic doping level-temperature phase diagram of the layered cuprates:



More or less understood are the undoped AF phase ($\delta \approx 0$) as a charge transfer insulator and the FL phase ($|\delta| > 0.2$) as a normal metal.

2. The undoped cuprate

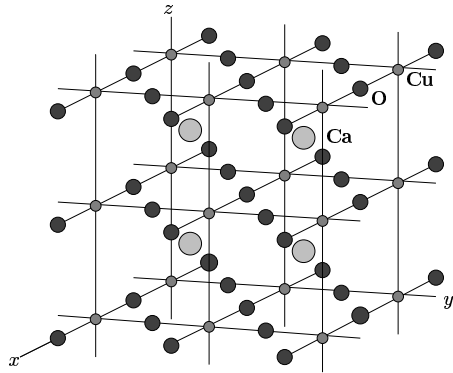
For $\delta = 0$, the valence electron number per unit cell of the $(\text{CuO}_2)^{2-}$ complex is $11 + 2 \times 4 + 2 = 21$ and hence odd.

The mean field band structure for an odd valence electron number per unit cell proposes a metallic state with a half-filled band at least above a possible spin magnetic order temperature.

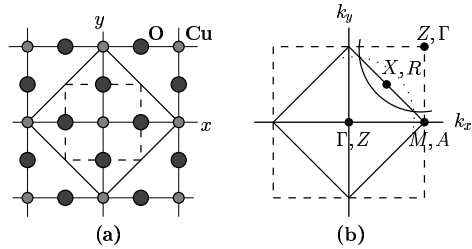
Experimentally the undoped cuprates are insulators with a gap of about 1 to 2 eV. Below the Néel temperature T_N which, dependent on the block layer, is between 250 and 540 K, they order antiferromagnetically with an ordered spin moment $\langle \mu \rangle (T \rightarrow 0)$ between 0.25 and $0.64 \mu_{\text{Bohr}}$ at the Cu site.

Order is due to magnetic interlayer coupling. A two-dimensional square lattice spin 1/2 Heisenberg antiferromagnet would have a Néel ground state with an ordered moment of $0.307g\mu_{\text{Bohr}}$ where $g \approx 2$ is the Landé factor, but would not order at $T > 0$; it would only develop local AF correlations.

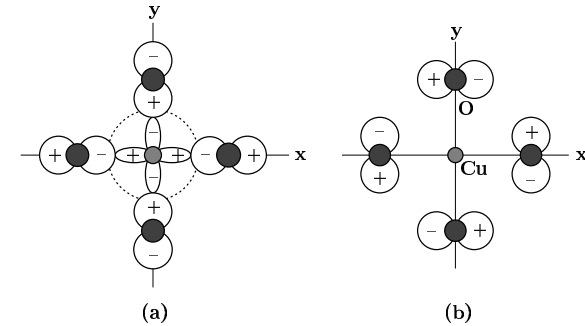
2.1. CaCuO_2 as an $n = \infty$ model cuprate



B is absent.
 In reality, $\text{Ca}_{0.85}\text{Sr}_{0.15}\text{CuO}_2$ has been synthesized which is an AF insulator with the highest Néel temperature, $T_N \approx 540$ K, of all cuprates and which hardly can be doped. However, the isostructural electron doped compound $\text{Sr}_{1-x}\text{Nd}_x\text{CuO}_2$, $x \leq 0.16$, was reported to be superconducting with T_c up to 40 K.



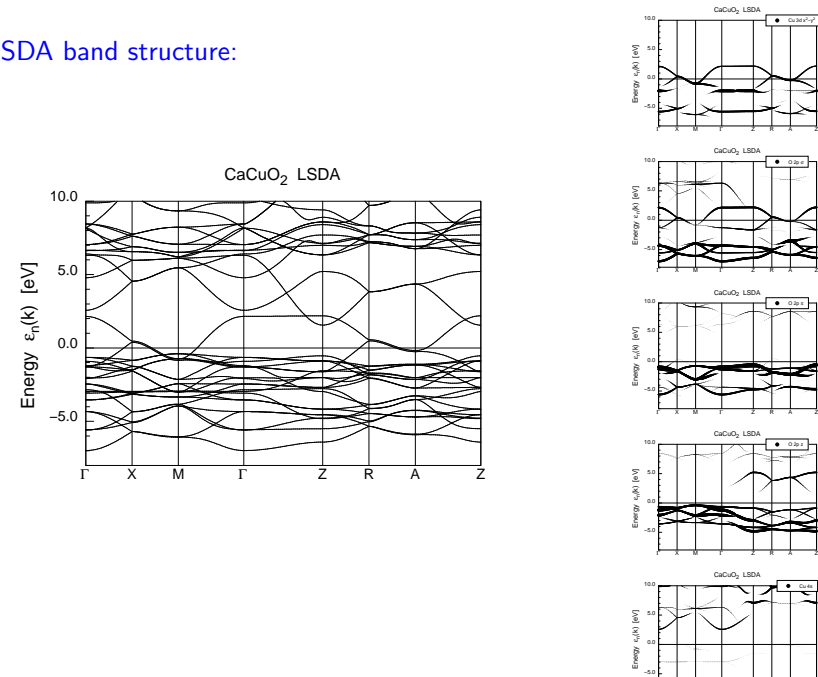
The planar CuO_2 structure. Non-magnetic (dashed line) and antiferromagnetic (full line) unit cell (a) and BZ (b). In the AF unit cell the copper spin in the center of the cell is 'up' and in the corners 'down'. The labeling of symmetry points in (b) is for the antiferromagnetic zone; the first label is for $k_z = 0$ and the second for $k_z = \pi$, X: $(k_x, k_y) = (\pi/2, \pi/2)$, M: $(k_x, k_y) = (\pi, 0)$ (in units of $1/c$ and $1/a$). The solid curve in the right upper quadrant sketches the mean-field FS of the non-magnetic state which consists of rods around the lines $(\pm\pi, \pm\pi, k_z)$. The dotted curve sketches its back folded image in the magnetic BZ.



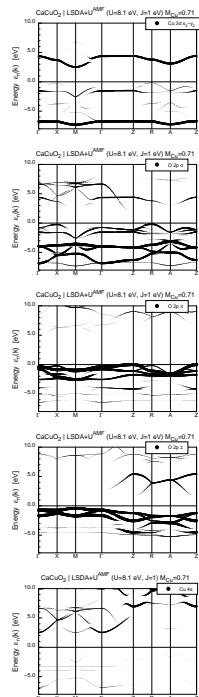
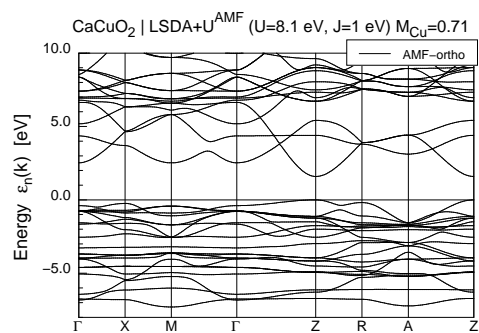
The relevant orbital combinations at $(k_x, k_y) = (\pi, \pi)$ of the non-magnetic BZ which is equivalent to $(k_x, k_y) = (0, 0)$ of the antiferromagnetic zone.

Oxygen $2p$ -orbitals having their lobes in the direction of the Cu-O bond are called $2p_\sigma$ orbitals ($(m = 0)$ -orbitals with respect to the bond direction as quantization axis), and those having their lobes perpendicular to the bond direction are called $2p_\pi$ orbitals ($(|m| = 1)$ -orbitals). Antibonding means a wavefunction node (sign change) intersecting the bond, bonding means no such node. (a) Full line: the antibonding $\text{Cu}-3d_{x^2-y^2}-\text{O}-2p_\sigma$ orbital combination of B_{1g} symmetry of the point group D_{4h} ; dotted: the $\text{Cu}-4s$ orbital of A_{1g} symmetry. (b) The O-O antibonding $2p_\pi$ orbital combination of A_{2g} symmetry.

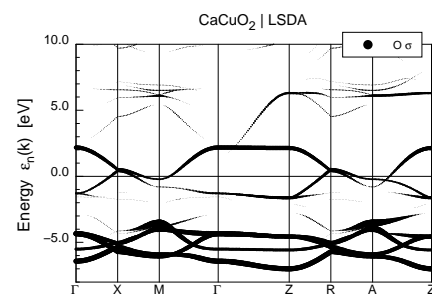
LSDA band structure:



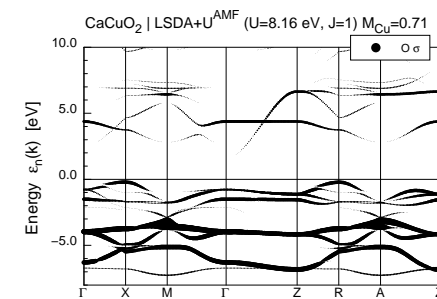
LSDA+ U band structure:



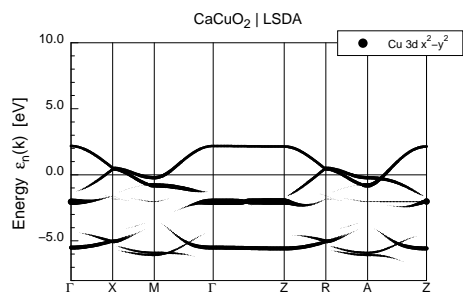
LSDA



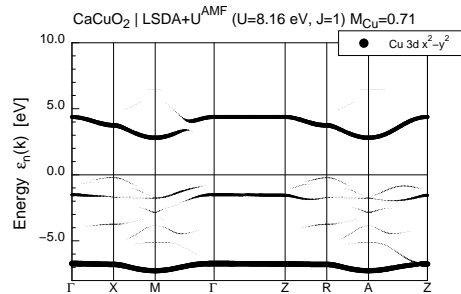
LSDA+ U



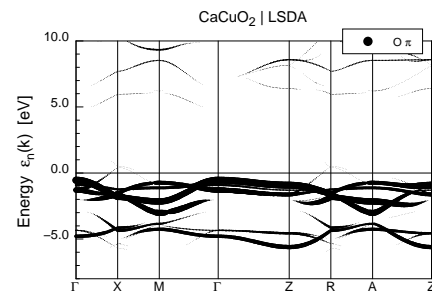
LSDA



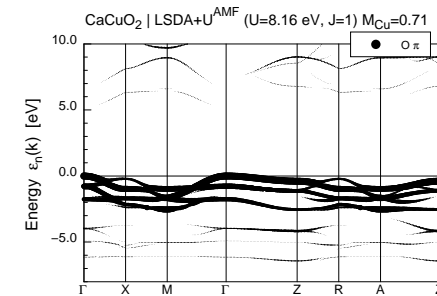
LSDA+ U



LSDA



LSDA+ U



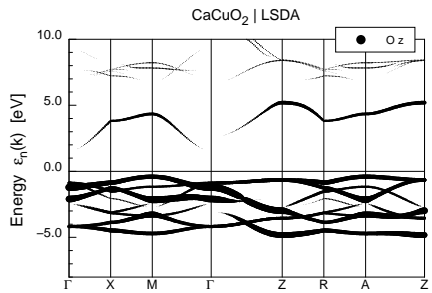
3. Theoretical models

Emery model: (Hole picture, that is the energy axis reversed compared to the previous band structures)

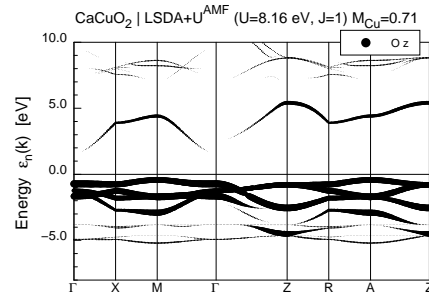
$$\hat{H} = \epsilon_d \sum_i \hat{n}_i^d + \epsilon_p \sum_j \hat{n}_j^p - t_{dp} \sum_{\langle ij \rangle, \sigma} (\hat{p}_{j\sigma}^\dagger \hat{d}_{i\sigma} + \hat{d}_{i\sigma}^\dagger \hat{p}_{j\sigma}) - t_{pp} \sum_{\langle jj' \rangle, \sigma} \hat{p}_{j'\sigma}^\dagger \hat{p}_{j\sigma} + U_d \sum_i \hat{n}_{i\uparrow}^d \hat{n}_{i\downarrow}^d + U_p \sum_j \hat{n}_{j\uparrow}^p \hat{n}_{j\downarrow}^p + U_{dp} \sum_{\langle ij \rangle} \hat{n}_j^p \hat{n}_i^d.$$

Standard parameters (in eV) are $\epsilon_p - \epsilon_d = 3.6$, $t_{dp} = 1.3$, $t_{pp} = 0.65$, $U_d = 10.5$, $U_p = 4$, $U_{dp} = 1.2$.

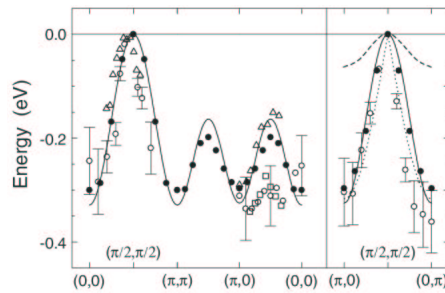
LSDA



LSDA+U



2.2. Angle resolved photoemission spectroscopy on Sr₂CuO₂Cl₂



Energy dispersion of quasiparticles for Sr₂CuO₂Cl₂. The energy zero is put at the top of the band, about 0.7 eV below Fermi level. Open symbols: experimental data; solid circles: self-consistent Born approximation for a $t - t' - t'' - J$ model; solid line: tight-binding fit; dashed: $t - J$ model; dotted: spinon model dispersion. (Reprinted with permission from Tohyama and Maekawa 2000.)

The undoped cuprates have one d -hole per Cu atom which sits in the lower hole Hubbard d -band (unoccupied upper electron Hubbard).

The next band in energy is predominantly of oxygen character without holes present (highest occupied electron band).

One therefore tries to mimic this charge transfer excitation case by an **effective one-band Hubbard model**:

$$\hat{H} = -t \sum_{\langle ii' \rangle, \sigma} (\hat{c}_{i\sigma}^\dagger \hat{c}_{i'\sigma} + \hat{c}_{i'\sigma}^\dagger \hat{c}_{i\sigma}) + U \sum_i \hat{n}_{i\uparrow} \hat{n}_{i\downarrow}.$$

The parameters (again in eV) to reproduce closely the low energy spectrum of the Emery model are $t = 0.43$ and $U = 5.4$.

In the subspace of the state space of avoided double occupancies of Cu sites by holes, the one-band Hubbard model may be canonically transformed into the $t - J$ Hamiltonian: (with some three-center terms neglected)

$$\hat{H} = -t \sum_{\langle ii' \rangle, \sigma} (\hat{C}_{i'\sigma}^\dagger \hat{C}_{i\sigma} + \hat{C}_{i\sigma}^\dagger \hat{C}_{i'\sigma}) + J \sum_{\langle ii' \rangle} (\mathbf{S}_{i'} \cdot \mathbf{S}_i - \frac{1}{4} \hat{n}_{i'} \hat{n}_i),$$

where $\hat{C}_{i\sigma} = \hat{c}_{i\sigma}(1 - \hat{n}_{i-\sigma})$, $J = 4t^2/U$, and \mathbf{S}_i is a spin-1/2 operator at site i .

At half-filling, $n_{i-\sigma} = 1$, the $t - J$ Hamiltonian reduces to the **square lattice Heisenberg Hamiltonian**:

$$\hat{H} = J \sum_{\langle ii' \rangle} \mathbf{S}_{i'} \cdot \mathbf{S}_i.$$

The ground state of the latter is now known to be the AF Néel state. It is, however, assumed that the Néel ground state is nearly degenerate with a nearest neighbor resonating valence bond state (RVB) in which neighboring copper spins form singlets ('valence bond singlets').

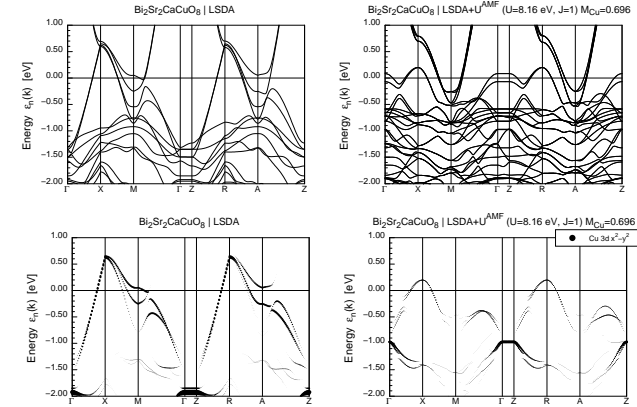
4. Doped cuprates

The cuprates of families (i) and (ii) may be doped continuously from the AF insulator at $\delta \approx 0$ into (and eventually beyond) the superconducting state, family (i) with both signs of δ .

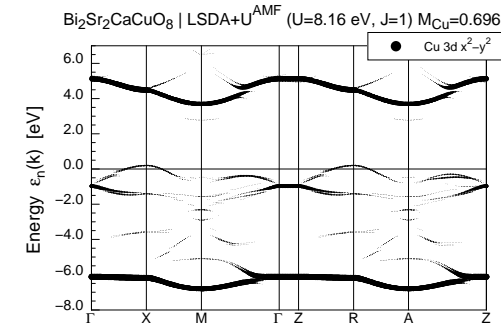
At low doping the spectra show broad features not crossing the Fermi level and still reminiscent of the AF symmetry of the BZ, before a FS according to the full line of Fig. 3b starts to develop, in the hole doped case beginning near $(\pi/2, \pi/2)$.

4.1. Overdoped regions

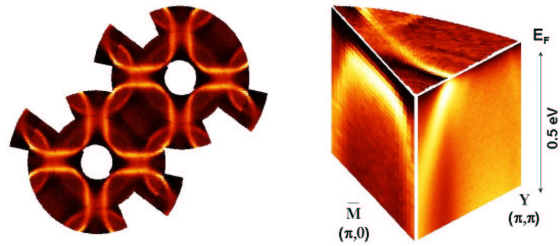
LSDA and LSDA+ U band structure of $\text{Bi}_2\text{Sr}_2\text{CaCu}_2\text{O}_8$:



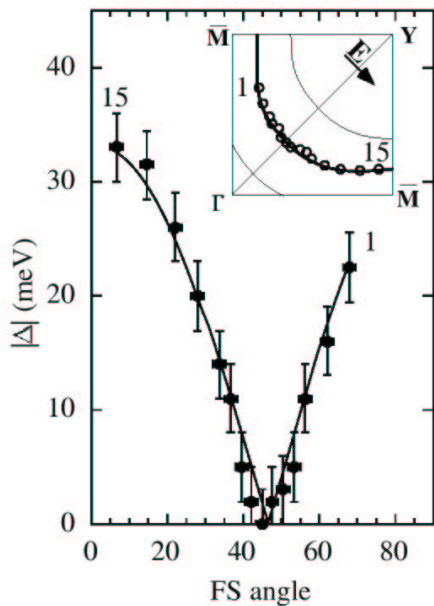
Left: LSDA, right: LSDA+ U , top: all bands, bottom: $\text{Cu}3d_{x^2-y^2}$ projected bands.



The $\text{Cu}3d_{x^2-y^2}$ projected bands of the LSDA+ U band structure of $\text{Bi}_2\text{Sr}_2\text{CaCu}_2\text{O}_8$



Color plot of ARPES intensity from overdoped $(\text{Bi,Pb})_2\text{Sr}_2\text{CaCu}_2\text{O}_{8+x}$. Left panel: Momentum distribution at the Fermi energy taken at 300 K and showing the hole FS rods around (π, π) (center of the dark area, called Y in the right panel) and the 'shadow FS' rods around $(0, 0)$ (center of the white spots) possibly due to AF correlations still present. Right panel: energy and momentum distribution showing also the dispersion of the bands. (By courtesy of J. Fink.)



By very high energy resolution ARPES ($\Delta E \sim 10\text{meV}$) the gap function $|\Delta(\mathbf{k})|$ on the FS of the superconducting state well below T_c is measured. A d -wave order parameter

$$\Delta(\mathbf{k}) = \Delta_0 [\cos(k_x a) - \cos(k_y a)]$$

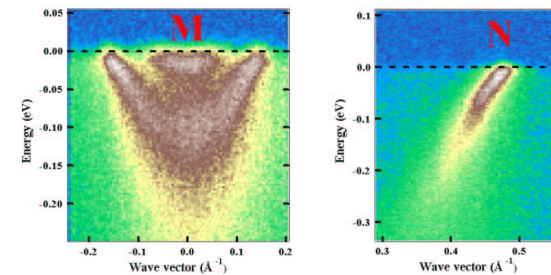
is found.

Superconducting gap measured at 13 K on $\text{Bi}_2\text{Sr}_2\text{CaCu}_2\text{O}_{8+x}$ ($T_c = 87\text{ K}$) and plotted vs. the angle along the normal-state FS, together with a d -wave fit. (Reprinted with permission of Ding *et al.* from *Phys. Rev. B* **54**, 9678 (1996).)

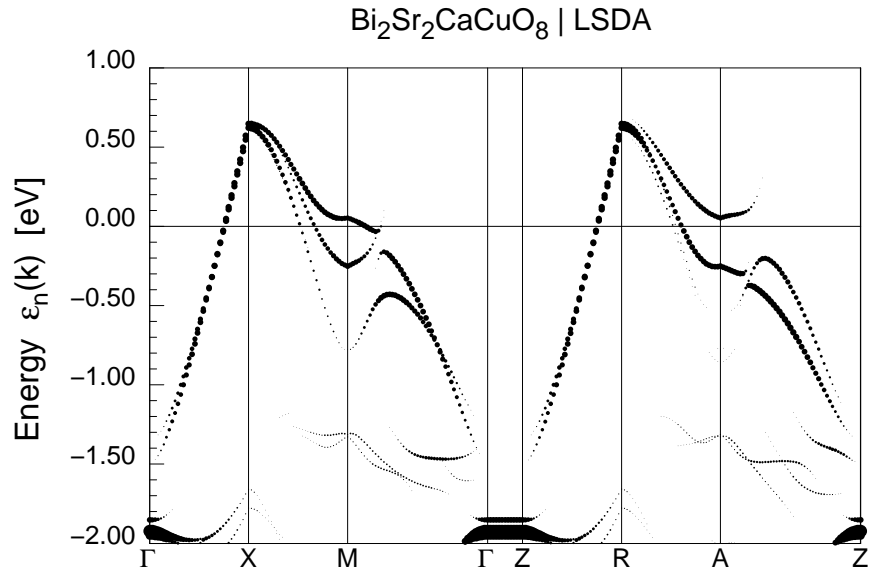
4.2 Bilayer splitting in $(\text{Bi,Pb})_2\text{Sr}_2\text{CaCu}_2\text{O}_{8+\delta}$

In the cuprate families (ii) and (iii) for $n > 1$, there are stacks of n CuO_2 -layers which in mean-field theory appear electronically coupled across the cation C layers even if (as is generally the case) the coupling across the block layers is negligible. It leads to an n -fold splitting of the conduction band of the CuO_2 -layers which also survives various (but maybe not all) many-body approaches. For symmetry reasons this splitting is zero for $k_x = k_y$ and maximal at $(\pi, 0)$. It seems to have the symmetry of the superconducting order parameter which led to speculations in the literature. However, one must be cautious with this type of behavior of a number of features; it may simply be related to the mirror plane $k_x = k_y$ of the point symmetry of the crystal and need not be caused by superconducting correlations (which of course are also connected with this symmetry).

In particular for $n = 2$ there is a bilayer splitting ($\sim 300\text{ meV}$ in LDA) which in the case of $(\text{Bi,Pb})_2\text{Sr}_2\text{CaCu}_2\text{O}_{8+\delta}$ has been intensively studied with ARPES and clearly found in overdoped samples at $(\pi, 0)$ with a value of 90 meV .



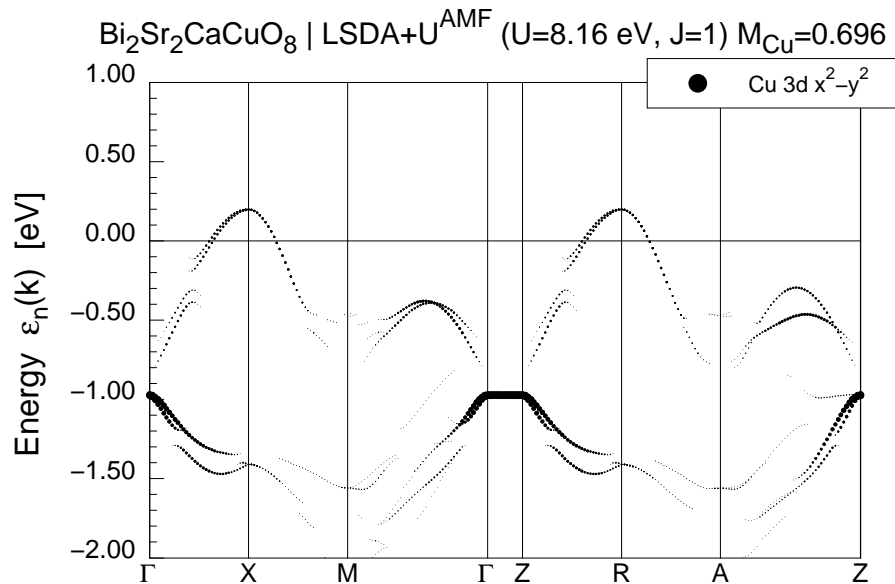
Color plot of ARPES energy-momentum distributions from overdoped $(\text{Bi,Pb})_2\text{Sr}_2\text{CaCu}_2\text{O}_{8+x}$ in the superconducting state at 30 K; left panel: near $(\pi, 0)$ showing the bilayer splitting of the bands; right panel: non-split band near the nodal point $k_x = k_y$ (N) of the FS. (By courtesy of J. Fink.)



4.3 Underdoped region

The underdoped region of hole doping has been intensively studied because of two striking features (which might be related): the [pseudogap](#) and the [stripe phase](#) (see Tohyama and Maekawa 2000). It was found in many cuprates but was most intensively studied in Bi₂Sr₂CaCuO_{8+δ} that in the underdoped region away from the nodal point $k_x = k_y$ the ARPES peak (which in this doping region often is merely a broad hump) does not cross the Fermi level but ends at a certain energy distance, the pseudogap value, from the latter. Often it seems to bend away from the Fermi level again like an AF folded band. It has again the symmetry with respect to $k_x = k_y$ mentioned in the last section.

Particularly in the cuprate family (i) but not exclusively there, incommensurate AF correlations close to $\mathbf{Q} = (\pi, \pi)$ are found which sometimes condense into incommensurate long-range order accompanied by incommensurate charge order. This might be caused by strong electron-lattice interaction leading to a separation into alternating AF and charged stripes.

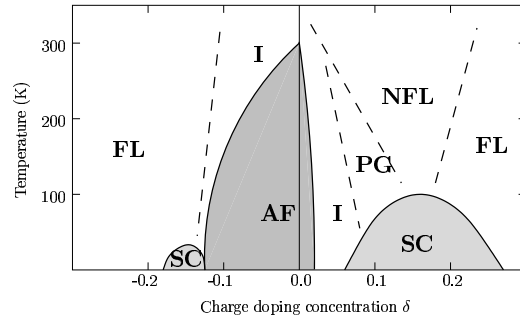


4.4 Single-electron self-energy

As was demonstrated by Norman *et al.* (1999), the self-energy of the single-electron Green's function can directly be extracted from ARPES data, if certain assumptions are made, namely that an extrinsic background can be properly subtracted and the electronic structure has particle-hole symmetry in the close vicinity of the FS point considered.

Earlier ARPES studies of the self-energy focused on the $(\pi, 0)$ point which, however, is masked by bilayer splitting. Recently, a number of investigations (cf. Damascelli *et al.* 2003) at the nodal point $k_x = k_y$ revealed a [linear temperature dependence of the imaginary part of the self-energy](#) at optimal doping, which seems to correspond to the linear temperature dependence of the scattering rate in normal state resistivity, but which in the ARPES results extends deep into the superconducting state. This would be consistent with the [marginal FL model](#) (Varma 1997).

5. Summary



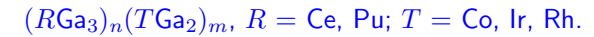
The electronic structure of cuprate superconductors is more or less settled in the cases of undoped ($\delta \approx 0$) and overdoped ($|\delta| \gtrsim 0.2$) material. In the former case it is that of an AF charge transfer insulator which can theoretically be described by a $t - J$ -model Hamiltonian. It might be necessary to incorporate in-plane $O-2p_\pi$ orbitals into this model for certain considerations. In the overdoped case, a weakly renormalized LDA band structure of a $Cu-3d_{x^2-y^2}-O-2p_\sigma$ band is experimentally found in the vicinity of the Fermi level in ARPES.

At optimal doping ($\delta \approx 1/6$) for superconductivity, experimental evidence seems to accumulate for a marginal FL state at elevated temperature, which is masked by the d -wave superconducting state at low temperature.

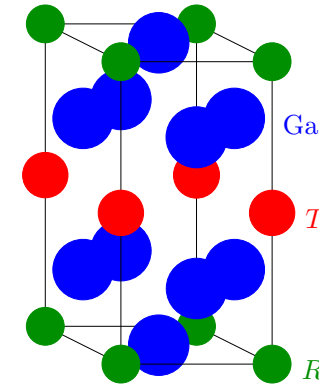
Still largely unclear is the situation in the underdoped region where several interactions seem to be interwoven leading to a complex behavior.

6. Appendix

Another family of stacked superconductor structures is



Structure:



Nature 420/21 297 (2002):

